


Constant potentials in 6D Einstein-Gauss-Bonnet theory

Sudan Hansraj^{Ⓜ,*}, Sunil D. Maharaj^{Ⓜ,†} and Brian Chilambwe[‡]

*Astrophysics and Cosmology Research Unit, School of Mathematics, Statistics and Computer Science,
University of KwaZulu-Natal, Private Bag X54001, Durban 4000, South Africa*

 (Received 23 August 2019; published 11 December 2019)

The qualitative physical behavior of six-dimensional perfect fluid spheres is studied in the context of Einstein-Gauss-Bonnet (EGB) gravity theory, and a contrast is drawn with the associated Einstein model. At first we seek an analogue of the defective Einstein universe by setting the temporal potential to be constant. The equation of state $\rho + \frac{5}{3}p = \alpha$, a constant multiple of the Gauss-Bonnet coupling α is obtained, and in the case of vanishing α the six-dimensional Einstein universe is recovered. More significantly the case of a constant spatial potential generated an exact solution in terms of hypergeometric functions. No solution in terms of elementary functions was located; however it was still possible to construct a compact star with finite radius for a specific choice of potential and suitable parameter values obtained by fine-tuning. It emerged that the EGB model was singularity free and displayed a number of pleasing physical features which were extrapolated from the usual restrictions placed on Einstein spheres. It was found that the EGB higher curvature terms allowed for the existence of stellar radius some 20 times larger than its Einstein counterpart. Moreover, the Einstein model suffered the permanent defect of a central singularity. In many respects the Gauss-Bonnet offered corrections to the corresponding Einstein model.

DOI: [10.1103/PhysRevD.100.124029](https://doi.org/10.1103/PhysRevD.100.124029)

I. INTRODUCTION

Einstein's general theory of relativity is still celebrated as the most successful theory of the gravitational field. Indeed the theory satisfies all reasonable experimental tests and has recently received additional support by the discovery of gravitational waves—a long-standing conjecture of Einstein [1]. However, the theory still lacks the ability to explain certain fundamental observations concerning the evolution of celestial phenomena. For example, the accelerated expansion of the Universe is not a direct consequence of general relativity, yet this fact has been credibly confirmed by Wilkinson microwave anisotropy probe [2,3] surveys. In order to explain these observations in the context of general relativity, some have invoked the cosmological constant while others have punted dark energy with a negative pressure gradient necessary to drive inflation. It is believed that dark energy constitutes about three-quarters of the energy budget of the Universe; however, its existence is unconfirmed at present. As for the cosmological constant, anomalies exist between its value predicted by quantum field theory and the astronomically observed values. To address this problem Ellis [4,5] has proposed the use of the trace-free Einstein equations—a theory equivalent to that of unimodular gravity [6]. These

directions demonstrate that questions still exist around the true theory of gravity.

Could the resolution of these questions lie in the realm of geometry since gravity is known to be a geometrical effect on large scales as opposed to a classical force? Pursuing this direction, various modifications of the fundamental theory have been made. Lovelock [7,8] postulated a remarkable action principle consisting of a polynomial with terms quadratic in the Riemann tensor, Ricci tensor, as well as the Ricci scalar but free of derivatives of the Riemann tensor and its contractions. Dadhich [9] has consistently argued that the pure Lovelock equations constitute the true theory of gravity. In the most general N th order Lovelock polynomial it is found that second order equations of motion are realizable for any spacetime dimension d . A major advantage of Lovelock theory is that to first order it is exactly the Einstein theory—hence the gains of general relativity are not necessarily lost. Of course, the serious challenge of the Lovelock theory is the intractable system of differential equations it yields. The Einstein field equations are famously difficult to solve on account of their nonlinearity, and now with the addition of higher order terms the nonlinear situation is exacerbated. Moreover, higher curvature terms are only active in spacetime dimensions greater than 4 and the question of how these extra dimensions are topologically hidden is not resolved save to state that to second order the Lovelock polynomial is the Gauss-Bonnet term that occurs naturally in string theory where dimensions higher than 4 are

*hansrajs@ukzn.ac.za

†maharaj@ukzn.ac.za

‡brian@aims.ac.za

required for the viability of the theory. A return to four dimensions is possible by addition of a dilatonic scalar field, and this is termed EdGB theory. Early forays in this direction were made by Guo *et al.* who studied dilatonic Einstein-Gauss-Bonnet (EGB) black holes in various dimensions [10]. The quasinormal modes of EGB dilaton black holes were studied by [11]. Ripley and Pretorius [12] considered the subject of gravitational collapse in this area. Iihoshi [13] established that the Einstein frame requires modification in EdGB. Our interest though is on the six-dimensional Einstein-Gauss-Bonnet field equations. Recently Chow and Pang [14] constructed the first rotating string solution in six-dimensional EGB supergravity. Obtaining exact solutions to the system of partial differential equations, though difficult, is vitally important in investigating the dynamical evolution of fluids by the construction of physically viable models. Such fluid models are useful in increasing our understanding of cold planets, neutron stars and strange stars when higher curvature effects are at play.

Pure Lovelock gravity refers to the construction of field equations from a Lagrangian density consisting only of the N th order of the Lovelock polynomial. Several interesting results have emerged in this area and they affect our treatment of the full Lovelock gravity theory. Recently it was shown by Dadhich and coworkers [9,15] that there is a functional relationship between d and N for viable astrophysical and cosmological models in pure Lovelock gravity. For the case $d = 2N$ no exterior vacuum metric is possible. The critical dimensions are $d = 2N + 1$ and $d = 2N + 2$ ([16]). It has been shown in the pure Lovelock gravity regime [9,15] that in the odd dimension gravity is kinematic (in the sense that $R_{ab} = 0$ implies $R_{abcd} = 0$) while for $d \geq 2N + 1$ the equations of motion allow for dynamical behavior. There exist no nontrivial vacuum solutions in pure Lovelock theory for $d = 2N + 1$. The interior Schwarzschild metric (incompressible sphere) holds—and is independent of spacetime dimension d and order of Lovelock polynomial N . The isothermal fluid sphere with density behaving as $\frac{1}{r^N}$ and with equation of state (EOS) pressure proportional to density was examined, and it was found in [17] that a constant potential is a necessary and sufficient condition for the existence of isothermal spheres in pure Lovelock gravity. By design, the latter models are unphysical—having a singular center and not admitting a pressure-free boundary. Other compact distributions of perfect fluids were studied by [18]. Utilizing the metric ansatz of Finch and Skea regular fluid models were devised that satisfied all the elementary physical requirements for the demonstrated case $N = 2$, $d = 6$. (The $d = 5$ case amounted to an unbounded cosmological fluid as expected.) Notwithstanding the fact that to first order the Lovelock polynomial is simply the Einstein type containing only the Ricci scalar of order 1, some believe that this is a negative feature since the effects

of the higher curvature terms may not be switched off by setting some parameter to 0.

The pure Lovelock field equations for a perfect fluid source were reported in [17]. Scrutinizing the equations carefully reveals that the case $d = 2N + 1$ is a special case that eliminates a number of terms in the field equations. To allow for the Lovelock gravity to make its full effect known, it is desirable to examine the case $d > 2N + 1$. For the Gauss-Bonnet case ($N = 2$) the relevant dimensions are 5 and 6. Models of perfect fluid matter in five dimensions have been treated in [19–21]. In this work we study the crucial dimension $d = 6$, which allows for a greater contribution from the quadratic order Riemann tensor terms. The field equations are more complicated due to the survival of more nonlinear contributors. The Einstein-Gauss-Bonnet case has been extensively studied over the past three decades [22–24]. The exterior metric was established by Boulware and Deser [5]; however interior metrics were only reported recently [19–21,25] for the five-dimensional case. To date no six-dimensional perfect fluid metrics have been reported except the general result of Dadhich *et al.* [9] that the constant density Schwarzschild metric is universal for all values of d , and N . Novak *et al.* [26] have analyzed Gauss-Bonnet supergravity in six dimensions.

The physical requirements normally imposed on exact Einstein-Gauss-Bonnet models are extrapolated from the Einstein version and are as follows. It is expected that the density (ρ) and pressure (p) profiles of a compact object are positive definite. Further, we demand that a hypersurface of vanishing pressure should exist demarcating the boundary of the fluid. The lack of such a boundary would suggest the presence of an unbounded cosmological fluid. The weak, strong, and dominant energy conditions, $\rho - p > 0$, $\rho + p > 0$, and $\rho + 3p > 0$, should also be satisfied. In order for the fluid to be causal the condition $0 < \frac{dp}{d\rho} < 1$ should hold, thus ensuring that the sound speed is subluminal. Note that it is customary to use the standard Israel-Darmois junction conditions of general relativity for simplicity. The correct junction conditions for EGB have been discussed by Davis [27]; however, it still has to be reduced to a condition that can easily be imposed on the system.

The paper is arranged as follows. We commence by mentioning salient aspects of Einstein-Gauss-Bonnet theory and derive the associated field equations for a spherically symmetric spacetime in six dimensions coupled to a perfect fluid matter source with comoving velocity vector. The equations are then transformed to an equivalent form where the gravitational potentials are now expressed as y and Z to aid the integration. The constant and linear forms for both y and Z are then studied and exact models are obtained in each case. In addition note that the analogue of the Buchdahl upper bound for the mass-radius ratio of $\frac{4}{9}$ has been discussed in [28] and bounds on the quantity $\frac{M}{R^2}$

were obtained depending on the sign of the coupling constant for five-dimensional EGB. The situation in six-dimensional EGB has not been investigated to date. Nevertheless there is interest in the ratio $\frac{M}{R}$ since this ratio has the property of constraining the surface redshift in Einstein gravity to a value $z \leq 1$. According to [28] there is no equivalent bound for five-dimensional EGB, but the question remains open for the six-dimensional case.

II. EINSTEIN-GAUSS-BONNET GRAVITY

We require an adapted action, different from the Einstein case, to generate the field equations in EGB gravity. In this paper we are working in six dimensions. The Gauss-Bonnet action in six dimensions can be written as

$$S = \int \sqrt{-g} \left[\frac{1}{2} (R - 2\Lambda + \alpha L_{\text{GB}}) \right] d^6x + S_{\text{matter}}, \quad (1)$$

where the parameter α denotes the Gauss-Bonnet coupling constant. Note that the Lagrangian is quadratic in the geometric quantities: the Ricci tensor, Ricci scalar, and Riemann tensor. Observe that the equations of motion for this action are second order and quasilinear, which are distinguishing features in EGB gravity. This is an advantage when compared with other modified theories of gravity. The Gauss-Bonnet term L_{GB} is present for $n > 4$ but has no contribution for $n \leq 4$.

The field equations in EGB gravity can be written as

$$G_{ab} + \alpha H_{ab} = T_{ab}, \quad (2)$$

with the metric signature $(- + + + +)$. The tensor G_{ab} is the Einstein tensor in six dimensions. The Lanczos tensor H_{ab} can be expressed in the form

$$H_{ab} = 2(RR_{ab} - 2R_{ac}R_b^c - 2R^{cd}R_{acbd} + R_a^{cde}R_{bcde}) - \frac{1}{2}g_{ab}L_{\text{GB}}. \quad (3)$$

The Lovelock term is defined by

$$L_{\text{GB}} = R^2 + R_{abcd}R^{abcd} - 4R_{cd}R^{cd}, \quad (4)$$

which combines the Ricci scalar, Ricci tensor, and Riemann tensor. The presence of the L_{GB} term greatly increases the nonlinearity and complexity of the field equations.

III. FIELD EQUATIONS

We are concerned with pseudo-Riemannian manifolds in six dimensions. The six-dimensional line element for static spherically symmetric spacetimes is taken as

$$ds^2 = -e^{2\nu} dt^2 + e^{2\lambda} dr^2 + r^2(d\theta^2 + \sin^2\theta d\phi^2 + \sin^2\theta \sin^2\phi d\psi^2 + \sin^2\theta \sin^2\phi \sin^2\psi d\eta^2), \quad (5)$$

where $\nu(r)$ and $\lambda(r)$ are arbitrary functions representing the gravitational field with coordinates $(x^a) = (t, r, \theta, \phi, \psi, \eta)$. We use the timelike comoving fluid velocity $u^a = e^{-\nu}\delta_0^a$ with the property $u^a u_a = -1$. The matter field is defined by the energy momentum tensor

$$T_{ab} = (\rho + p)u_a u_b + p g_{ab}, \quad (6)$$

where ρ and p are the energy density and isotropic pressure, respectively.

Then the EGB field equations (2) may be written in the form

$$\rho = \frac{1}{e^{4\lambda} r^4} [(4r^3 e - 48\alpha r(1 - r e^{2\lambda}))\lambda' - 6r^2 e^{2\lambda}(1 - e^{2\lambda}) + 12\alpha(e^{2\lambda} - 1)^2], \quad (7)$$

$$p = \frac{1}{e^{4\lambda} r^4} [(1 - e^{2\lambda})(6r^2 e^{2\lambda} - 48\alpha r\nu' + 12\alpha e^{2\lambda} - 12\alpha) + 4r^3 e^{2\lambda}\nu'], \quad (8)$$

$$0 = (1 - e^{2\lambda})[e^{2\lambda}(3r^2 + 12\alpha - 1) - 12\alpha r(3\nu' + \lambda')] + 12\alpha r^2(\nu'' + \nu'^2 - \nu'\lambda') + e^{2\lambda}[r^3(\nu' + 3\lambda') - r^4(\nu'' + \nu'^2 - \nu'\lambda')] - 24\alpha r^2\nu'\lambda' \quad (9)$$

in the canonical spherical coordinates (x^a) . Equation (9) is the equation of pressure isotropy. Note that the system (7)–(9) consists of three field equations in four unknowns, which is similar to the standard Einstein case for spherically symmetric perfect fluids. However the nonlinearity in the system (7)–(9) has now greatly increased because of the presence of the EGB coupling parameter α . The presence of terms containing α makes the system more complex and difficult to solve in general.

We attempt to rewrite the system (7)–(9) in a simpler form by utilizing new coordinates due to Durgapal and Bannerji [29]. The coordinate change $x = Cr^2$, $e^{2\nu} = y^2(x)$, and $e^{-2\lambda} = Z(x)$ converts Eqs. (7)–(9) to the form

$$\frac{48\alpha Cx(Z-1)\dot{Z} - 4x^2\dot{Z} - 6x(Z-1) + 12\alpha C(Z-1)^2}{x^2} = \frac{\rho}{C}, \quad (10)$$

$$\frac{(96\alpha Cx(1-Z) + 8x^2)Z\dot{y} + (Z-1)(6x + 12\alpha C(1-Z))y}{x^2 y} = \frac{p}{C}, \quad (11)$$

$$4x^2Z(x + 3\beta[1 - Z])\dot{y} + 2x(x^2\dot{Z} + 3\beta[(1 - 3Z)\dot{Z}x - 2Z(1 - Z)])\dot{y} + 3((\beta(1 - Z) + x)(\dot{Z}x - Z + 1))y = 0, \quad (12)$$

which govern the structure of static stars in six-dimensional EGB theory. We have redefined $\beta = 4\alpha C$. As presented in Eq. (12) the isotropy equation has been written as a linear second order differential equation in y (if Z is a known quantity). This is the major advantage of the coordinate transformation invoked above. An equivalent form of the condition of pressure isotropy is

$$[x^2(2x\dot{y} + 3y) + 3\beta x(2x\dot{y} + y - (6x\dot{y} + y)Z)]\dot{Z} - 3\beta[4x^2\ddot{y} - 4x\dot{y} - y]Z^2 + [x(4x^2\ddot{y} - 3y) + 24\alpha C(2x^2\ddot{y} - 2x\dot{y} - y)]Z + 3(x + \beta)y = 0, \quad (13)$$

the trade-off being that now Eq. (13) is a nonlinear first order differential equation in Z (if y is prescribed). Note that (13) is an Abel differential equation of the second kind. Our intention is to find exact solutions to the generalized pressure isotropy conditions (12) or (13) in the presence of α . When $\alpha = 0$ we find that (12) reduces to the simpler form

$$4x^2Z\dot{y} + 2x^2\dot{Z}\dot{y} + 3(1 + x\dot{Z} - Z)y = 0, \quad (14)$$

which is the pressure isotropy condition in six-dimensional Einstein gravity.

To integrate (12) or (13) we must make simplifying assumptions on the functional forms of y or Z . A similar approach was followed by Hansraj *et al.* [20], Chilambwe *et al.* [21] and Maharaj *et al.* [20] in five-dimensional EGB gravity. However, the field equations in the six-dimensional EGB case are fundamentally different and of higher complexity. Therefore, the integration method and the resulting exact solutions will be completely different in six dimensions. Currently there are no known six-dimensional solutions for a perfect fluid in EGB except for the universal Schwarzschild interior metric [9] and the vacuum solution of Boulware and Deser [30], which was generalized to include the effects of the electromagnetic field by Wiltshire [24].

IV. ANALOGUE OF THE EINSTEIN UNIVERSE

The simplest point of departure is the choice of constant temporal potential y as considered by Einstein in general relativity. Setting $y = a$ where a is a constant, (13) reduces to

$$(x + \beta(1 - Z))(1 + x\dot{Z} - Z) = 0. \quad (15)$$

Equation (15) leads to ostensibly two solutions,

$$Z = 1 + \frac{x}{4\alpha C}, \quad Z = 1 + c_1x, \quad (16)$$

which are actually equivalent and where c_1 is an arbitrary constant. The line element for this category of solution assumes the simple form

$$ds^2 = -a^2dt^2 + (1 + c_1Cr^2)^{-1}dr^2 + r^2(d\theta^2 + \sin^2\theta d\phi^2 + \sin^2\theta \sin^2\phi d\psi^2 + \sin^2\theta \sin^2\phi \sin^2\psi d\eta^2), \quad (17)$$

which is the six-dimensional version of the defective Einstein universe. For the metric (17), the density and pressure

$$\rho = 10Cc_1(6\alpha Cc_1 - 1), \quad p = 6Cc_1(1 - 2\alpha Cc_1), \quad (18)$$

respectively are both constant. This is unrealistic and discordant with the observed Universe. Nevertheless it may be observed that the equation of state

$$\rho + \frac{5}{3}p = 40C^2c_1^2\alpha \quad (19)$$

is in evidence. When $\alpha = 0$, (17) gives $\rho + \frac{5}{3}p = 0$ in Einstein gravity in six dimensions. The six-dimensional metric (17) is the Einstein static universe that was first found by Patel *et al.* [31]. We can therefore interpret (17) as the Einstein universe in EGB gravity with equation of state (19). Note the appearance of the Gauss-Bonnet coupling constant α in (17); it directly affects the gravitational behavior in this model.

V. LINEAR TEMPORAL POTENTIAL

To illustrate the difficulty of obtaining exact solutions in the present context, consider a linear choice for the potential y . Let

$$y = 1 + ax, \quad (20)$$

where a is constant. Then Eq. (13) assumes the form

$$x\dot{Z}(5ax^2 + 3x(3a\beta + 1) - 3\beta Z(7ax + 1) + 3) - 3Z(ax^2 + 6a\beta x + 2\beta + x) + 3(ax + 1)(\beta + x) + 3\beta(5ax + 1)Z^2 = 0. \quad (21)$$

This is an Abelian equation of the second kind, which is in general difficult to solve. However, Eq. (21) integrates as

$$(Z - 1)^{15}(-105abxZ + 21abx + 35ax^2 - 15bZ + 15b + 21x)^2 = C_1x^7, \quad (22)$$

a higher order polynomial algebraic equation, for which an explicit solution is not known in terms of Z . C_1 is an integration constant. This implicit form is unhelpful in developing a complete model as the expressions for Z are required to unravel the density and pressure. We therefore do not pursue this case further.

VI. CONSTANT SPACE POTENTIAL

A constant choice for the potential Z leads to a rich family of exact solutions. We make the choice

$$Z = k, \tag{23}$$

where $k \neq 1$ is a constant in our approach. The stellar structure equations (10)–(12) simplify to

$$\frac{3\beta(k-1)^2 - 6x(k-1)}{x^2} = \frac{\rho}{C}, \tag{24}$$

$$\frac{(24\beta x(1-k) + 8x^2)k\dot{y} + (k-1)(6x + 3\beta(1-k))y}{x^2 y} = \frac{p}{C}, \tag{25}$$

$$4kx(x(-3\beta k + 3\beta + x)\dot{y} + 3\beta(k-1)\dot{y}) + 3(k-1)(\beta(k-1) - x)y = 0, \tag{26}$$

where the pressure isotropy equation (26) is of hypergeometric form. The general solution of (26) is given by

$$y = A {}_2F_1 \left(\left[\frac{\sqrt{k} - \sqrt{k_1} - \sqrt{k_2}}{2\sqrt{k}}, \frac{\sqrt{k} + \sqrt{k_1} - \sqrt{k_2}}{2\sqrt{k}} \right], \left[\frac{\sqrt{k} - \sqrt{k_2}}{\sqrt{k}} \right], \frac{x}{3\beta(k-1)} \right) x^{1-\sqrt{\frac{k_2}{k}}} + B {}_2F_1 \left(\left[\frac{\sqrt{k} + \sqrt{k_1} + \sqrt{k_2}}{2\sqrt{k}}, \frac{\sqrt{k} - \sqrt{k_1} + \sqrt{k_2}}{2\sqrt{k}} \right], \left[\frac{\sqrt{k} + \sqrt{k_2}}{\sqrt{k}} \right], \frac{x}{3\beta(k-1)} \right) x^{1+\sqrt{\frac{k_2}{k}}, \tag{27}$$

where A and B are constants of integration and ${}_2F_1$ is the hypergeometric function and we have defined $k_1 = 4k - 3$, $k_2 = 5k - 1$ to shorten lengthy expressions. In the form (27) this exact solution has limited use to model realistic stars. Solutions in terms of elementary functions are desirable however elusive. Some values of k such as 1 , $\frac{1}{5}$, and $\frac{3}{4}$ should be inspected more closely as suggested by (27) in the hope of finding closed form solutions. Extensive empirical testing and a comparison with tables of known cases of hypergeometric functions reducing to elementary functions proved futile. Nevertheless, we note the consequences of some choices in what follows.

A. $k = 1$

In this case, the differential equation (26) is solved by $y = c_1 + c_2 x$ for suitable constants c_1 and c_2 . This case has been considered in (22) where the associated algebraic equation proved intractable.

B. $k = \frac{1}{5}$

With this prescription, Eq. (26) assumes the form

$$x^2(x+2)\dot{y} - 2x\dot{y} + (3x+2)y = 0 \tag{28}$$

with solutions expressible in terms of Legendre P and Q functions in the form

$$y = c_1 x P_{\frac{1}{2}(i+\sqrt{11})} \left(\frac{5x}{6\beta} + 1 \right) + c_2 x Q_{\frac{1}{2}(i+\sqrt{11})} \left(\frac{5x}{6\beta} + 1 \right), \tag{29}$$

where c_1 and c_2 are integration constants. Following lengthy fine-tuning, no physically reasonable solution

emerged. Note that the presence of complex numbers in (29) is not an impediment to constructing meaningful plots as such terms may cancel.

C. $k = \frac{3}{4}$

For this value of the spatial potential, solutions in terms of Legendre functions are again in evidence. These are given by

$$y = c_1 \sqrt{x} P_{-\frac{1}{2}-\frac{\sqrt{33}}{6}} \left(\frac{2x+3\beta}{2x} \right) + c_2 \sqrt{x} Q_{-\frac{1}{2}-\frac{\sqrt{33}}{6}} \left(\frac{2x+3\beta}{2x} \right), \tag{30}$$

and in this case the functions are real valued. However, exhaustive testing resulted in no viable solutions.

VII. SIX-DIMENSIONAL EINSTEIN MODEL

The Einstein case is not a special case of (27) since it is prohibited from setting $\beta = 0$. The case $\beta = 0$ corresponds to the six-dimensional model in standard Einstein gravity and must be treated from the original isotropy equation. The solution to the field equation (12) is then given by

$$y = Ax^{\frac{k+\sqrt{4k^2-3k}}{2k}} + Bx^{\frac{k-\sqrt{4k^2-3k}}{2k}} \tag{31}$$

for $Z = k$ and where A and B are integration constants. For $k < 0$ (which is inadmissible) or for $k \geq \frac{3}{4}$ the solution (32) has standard exponential form. However, for the window $0 < k \leq \frac{3}{4}$ the complex valued exponential forms may be expressed as elementary functions. Specializing to the case $Z = \frac{1}{2}$ gives

$$y = \sqrt{x} \left(A \sin\left(\frac{\log x}{\sqrt{2}}\right) + B \cos\left(\frac{\log x}{\sqrt{2}}\right) \right), \quad (32)$$

which facilitates comparison with the corresponding EGB dynamical quantities. The dynamical quantities density and pressure have the forms

$$\frac{\rho}{C} = \frac{3}{x}, \quad (33)$$

$$\frac{p}{C} = -\frac{\left(a_4 \tan\left(\frac{\log x}{\sqrt{2}}\right) + a_5\right)}{x \left(A \tan\left(\frac{\log x}{\sqrt{2}}\right) + B\right)}, \quad (34)$$

respectively. The sound speed squared and equation of state indicator assume the forms

$$\frac{dp}{d\rho} = \frac{2a_1 a_2 \sin\left(\frac{2\log x}{\sqrt{2}}\right) + a_3 \cos\left(\frac{2\log x}{\sqrt{2}}\right) + 3(A^2 + B^2)}{6 \left(A \sin\left(\frac{\log x}{\sqrt{2}}\right) + B \cos\left(\frac{\log x}{\sqrt{2}}\right)\right)^2}, \quad (35)$$

$$\frac{p}{\rho} = -\frac{a_4 \tan\left(\frac{\log x}{\sqrt{2}}\right) + a_5}{3 \left(A \tan\left(\frac{\log x}{\sqrt{2}}\right) + B\right)} \quad (36)$$

for the case $Z = \frac{1}{2}$. The adiabatic stability function for Einstein gravity is given by

$$\Gamma = \frac{\left(a_1 \tan\left(\frac{\log x}{\sqrt{2}}\right) + a_2\right) \left(2a_1 a_2 \sin\left(\frac{2\log x}{\sqrt{2}}\right) + a_3 \cos\left(\frac{2\log x}{\sqrt{2}}\right) + 3(A^2 + B^2)\right)}{-3 \left(A \sin\left(\frac{\log x}{\sqrt{2}}\right) + B \cos\left(\frac{\log x}{\sqrt{2}}\right)\right)^2 \left(a_4 \tan\left(\frac{\log x}{\sqrt{2}}\right) + a_5\right)} \quad (37)$$

while the gravitational surface redshift has the profile

$$z = \frac{1}{\sqrt{x} \left(A \sin\left(\frac{\log(x)}{\sqrt{2}}\right) + B \cos\left(\frac{\log(x)}{\sqrt{2}}\right)\right)} - 1. \quad (38)$$

The mass function as well as the compactification ratio simplify to

$$m = \sqrt{\left(\frac{x}{C}\right)^3}, \quad (39)$$

$$\frac{m}{r} = \frac{x}{C} \quad (40)$$

as functions of the radial coordinate x . The expressions governing the energy conditions take the form

$$\frac{\rho - p}{C} = \frac{2\sqrt{2} \left(a_2 \tan\left(\frac{\log x}{\sqrt{2}}\right) - a_1\right)}{x \left(A \tan\left(\frac{\log x}{\sqrt{2}}\right) + B\right)}, \quad (41)$$

$$\frac{\rho + p}{C} = \frac{2 \left(a_1 \tan\left(\frac{\log x}{\sqrt{2}}\right) + a_2\right)}{x \left(A \tan\left(\frac{\log x}{\sqrt{2}}\right) + B\right)}, \quad (42)$$

$$\frac{\rho + 3p}{C} = \frac{6\sqrt{2} \left(A - B \tan\left(\frac{\log x}{\sqrt{2}}\right)\right)}{x \left(A \tan\left(\frac{\log x}{\sqrt{2}}\right) + B\right)}, \quad (43)$$

and these are all expected to be positive everywhere inside the stellar distribution. In the above we have put $a_1 = A - \sqrt{2}B$, $a_2 = \sqrt{2}A + B$, $a_3 = A^2 + 4\sqrt{2}AB - B^2$,

$a_4 = A + 2\sqrt{2}B$, and $a_5 = B - 2\sqrt{2}A$ to simplify the expressions. In what follows we perform a graphical analysis of these quantities to analyze the impact of the higher curvature terms arising from the Gauss-Bonnet coupling.

VIII. PHYSICAL ANALYSIS

In view of the difficulty in finding exact solutions to the EGB system that are expressible as elementary functions, we consider a variety of values for Z in the hope of isolating one that yields a physically reasonable model. The particular choice $Z = \frac{1}{2}$ generates a model that satisfies most of the standard requirements for realistic behavior. Since the solution still contains hypergeometric functions, it is not feasible to exhibit the lengthy expressions for the dynamical quantities. The solution for $Z = \frac{1}{2}$, namely, (27), is substituted in (24) and (25) to yield the density and pressure. Then the sound speed squared is established with the aid of the formula $\frac{dp}{d\rho}$. The ratio of the pressure to density $\frac{p}{\rho}$ is taken to give an indication of the equation of state. Clearly this cannot be established explicitly in view of the presence of hypergeometric functions. Additionally the index $\Gamma = \left(\frac{\rho+p}{\rho}\right) \frac{dp}{d\rho}$ is known as the Chandrasekhar adiabatic stability limit in general relativity, and it is expected to have a value in excess of $\frac{4}{3}$ for a stable sphere. It is interesting to check the behavior of this quantity in the presence of extra spacetime dimensions and higher curvature effects. The surface gravitational redshift is computed with the formula $z = e^{-\nu} - 1$ in the usual way. The active gravitational mass of the six-dimensional sphere is calculated with the formula $\int \rho r^4 dr$. Another useful quantity in assessing the stability of a stellar distribution is the

compactification parameter $\frac{m}{r}$, which in the Einstein theory satisfies Buchdahl's upper bound of $\frac{M}{R} \leq \frac{4}{9}$ for a star of radius $r = R$ and mass M provided that the energy density is a monotonically decreasing function. Finally we study the weak energy condition $\rho - p$, strong energy condition $\rho + p$, and dominant energy condition $\rho + 3p$, which are all expected to be positive within the distribution. Note that these physical quantities investigated here are extrapolated from the Einstein theory. The actual sound speed, gravitational surface redshift, Buchdahl limit, and Chandrasekhar limit for EGB theory is still an active area of research. However, we include these in an effort to study the distortion induced by the higher curvature terms on the six-dimensional Einstein counterpart.

With regards to the applicable boundary conditions we utilize the junction conditions of the standard theory of gravity in the absence of explicit conditions for the EGB framework. These junction conditions include the vanishing of the isotropic particle pressure on a suitable hypersurface as well as the matching of the first and second fundamental forms. With an exact solution in terms of elementary functions it is easy to establish the values of the two necessary integration constants c_1 and c_2 in terms of the mass M and radius R of the six-dimensional hypersphere. In practice this is nontrivial in the current context in view of the fact that our exact solution is in terms of hypergeometric functions. Nevertheless, it is still possible to investigate the physical behavior of our model qualitatively through graphical plots. From the plots we observe for example that surfaces of zero pressure certainly exist for our choice of parameters. This gives us confidence that the model has good prospects to conform to actual observations in relativistic astrophysics. For the purposes of our graphical analysis it was necessary to separate the Einstein versions ($\beta = 0$) from the Einstein-Gauss-Bonnet plots (β nonzero) in view of the discrepancy of the scales of the axes for identical chosen parameter values. We have utilized the parameter values $A = 10^{10}$, $B = 1$, $C = 1$ and constructed plots for $\beta = 10, 1, 0.1, 0.01$, which correspond respectively to the Gauss-Bonnet coupling constant values $\alpha = 2.5, 0.25, 0.025, 0.0025$ recalling the redefinition $\beta = 4\alpha C$ made earlier.

From Fig. 1 it is observed that the energy density is positive and monotonically decreasing for all values of β . The isotropic particle pressure p (Fig. 2) behaves similarly but in addition has the property that it vanishes for a finite radial value. This establishes the radius of the six-dimensional hypersphere. Specifically we observe the thick solid graph $\beta = 0.1$, which turns out to display behavior mostly consistent with the expectations of the dynamical quantities in general relativity. In this case the vanishing pressure hypersurface exists at $x = 0.02$ or $r = 0.1414$.

The sound speed should be subluminal and this translates to the requirement $0 < \frac{dp}{d\rho} \leq 1$. According to Fig. 3 this condition is satisfied in all cases but the case $\beta = 0.001$.

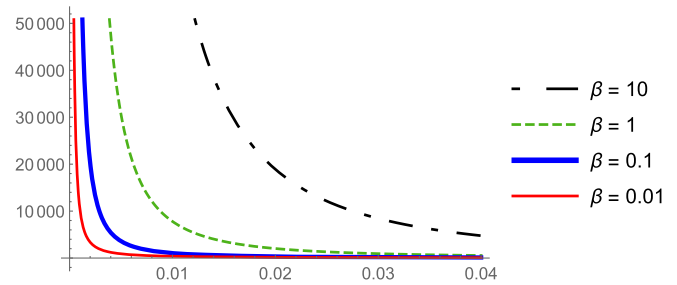


FIG. 1. EGB: Density ρ variation against radial value x .

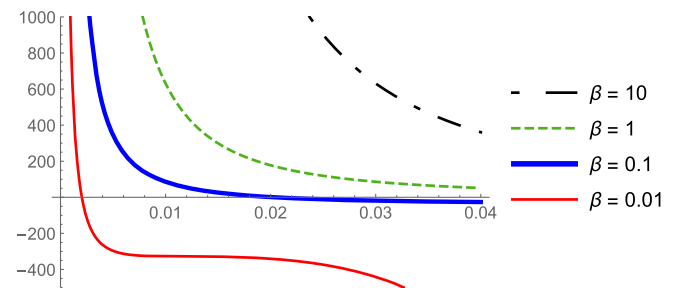


FIG. 2. EGB: Pressure p variation against radial value x .

The ratio $\frac{p}{\rho}$ gives an indication of the EOS within the star. For the case $\beta = 0.1$ it can be noted from Fig. 4 that the EOS is a smooth well-behaved function with no singularities inside the sphere. It is evident from Fig. 5 that for all values of β the Chandrasekhar adiabatic stability criterion

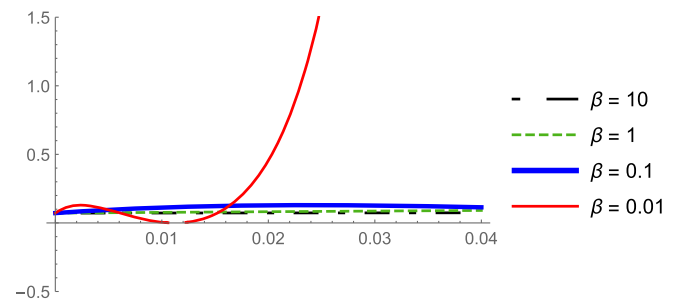


FIG. 3. EGB: Square of sound speed variation against radial value x .

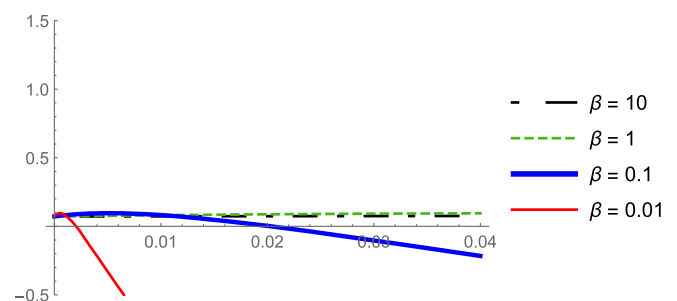


FIG. 4. EGB: Equation of state profile $\frac{p}{\rho}$.

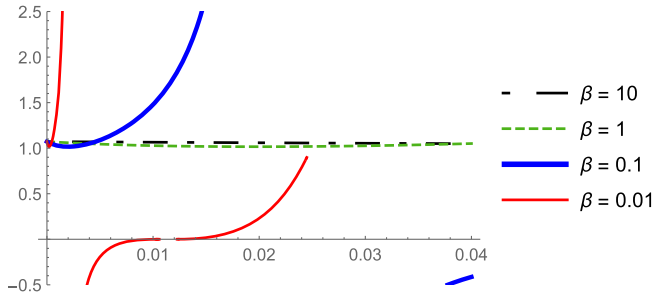


FIG. 5. EGB: Adiabatic stability parameter $\Gamma = \frac{(\rho+p)}{p} \frac{dp}{d\rho}$ variation against radial value x .

$\Gamma \geq \frac{4}{3}$ is violated. This suggests that this requirement may need modification to take into account the effects of the extra curvature induced by the Gauss-Bonnet terms. Another drawback of the model is that the surface redshift function (Fig. 6) appears to have a value very close to -1 and accordingly is interpreted as exhibiting blue-shift of light. This prevents an identification of the present model with known compact objects such as neutron stars or to more dense counterparts such as strange stars.

The active gravitational mass for all radial values is a smooth and increasing function in general as depicted in Fig. 7. The compactification ratio $\frac{m}{r}$ shown in Fig. 8 exhibits values lower than the Buchdahl upper bound of $\frac{4}{9}$ ($\equiv 0.444$) at least for the cases $\beta = 0.1$ and 0.01 , suggesting that the Buchdahl limit may be valid despite

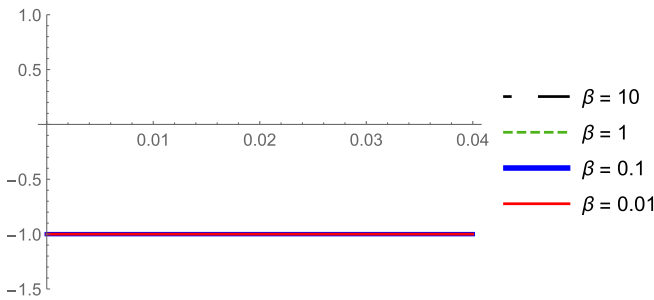


FIG. 6. EGB: Gravitational surface redshift variation against radial value x .

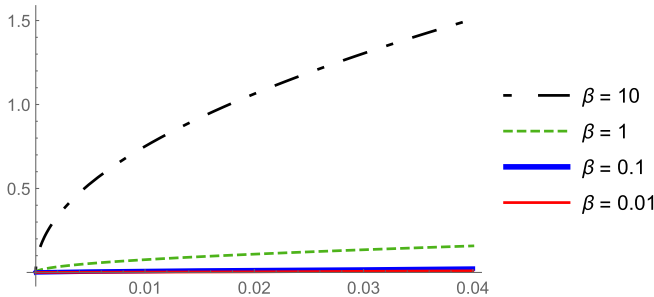


FIG. 7. EGB: Gravitational mass variation against radial value x .

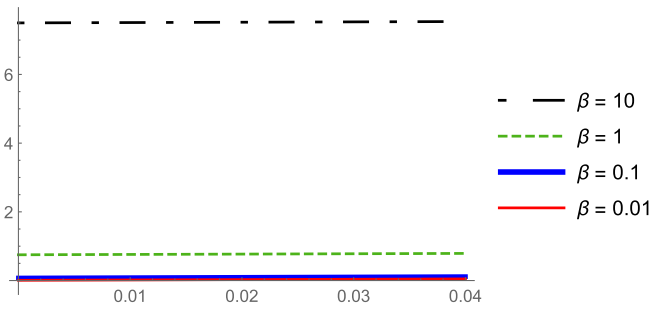


FIG. 8. EGB: Compactification parameter $\frac{m}{r}$ against radial value x .

higher curvature effects. Finally Figs. 9–11 display the energy conditions and it is clear that the weak, strong, and dominant energy conditions are all satisfied for the range of β values studied.

A comparison of the Einstein ($\beta = 0$) models with the EGB models incorporating higher curvature terms is also instructive. At the outset one undesirable and persistent feature in the Einstein framework is a singularity at the center of the distribution. Figure 12 demonstrates that the energy density and pressure are indeed both positive; however there exists a surface of vanishing pressure at a radius substantially smaller than the EGB version (Fig. 2) at approximately $x = 0.001$. The sound speed is mostly superluminal within the Einstein six-dimensional sphere as shown in Fig. 13. This same plot also depicts the equation of state function, which is smooth for $0 < x \leq 0.001$;

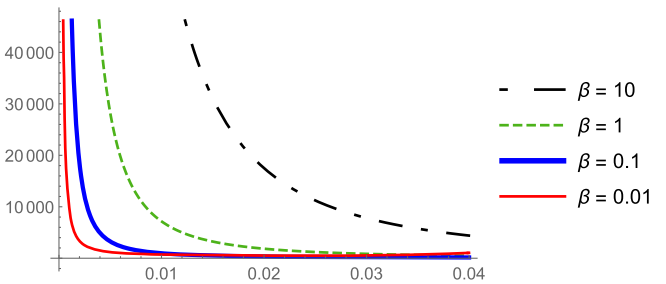


FIG. 9. EGB: Weak energy condition $\rho - p$ variation against radial value x .

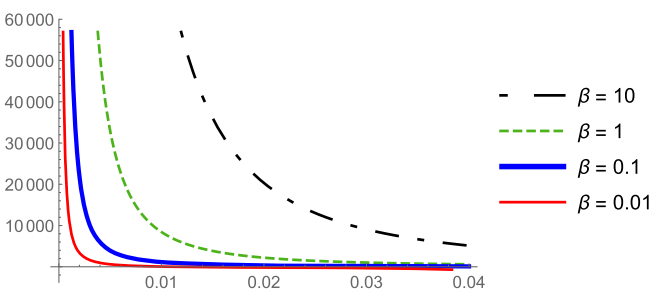


FIG. 10. EGB: Strong energy condition $\rho + p$ variation against radial value x .

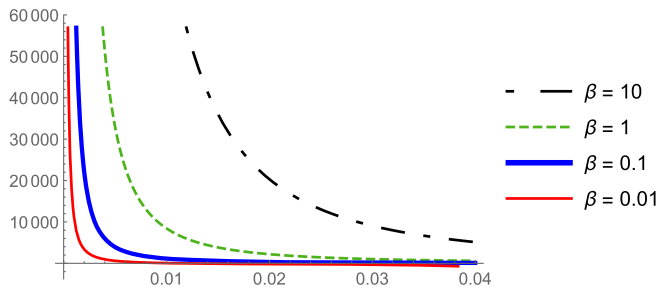


FIG. 11. EGB: Dominant energy condition $\rho + 3p$ variation against radial value x .

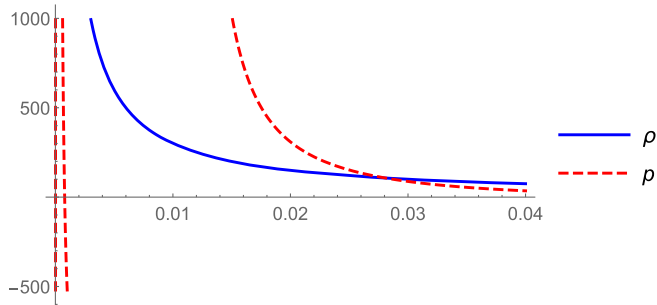


FIG. 12. Einstein: Density ρ and pressure p variation against radial value x .

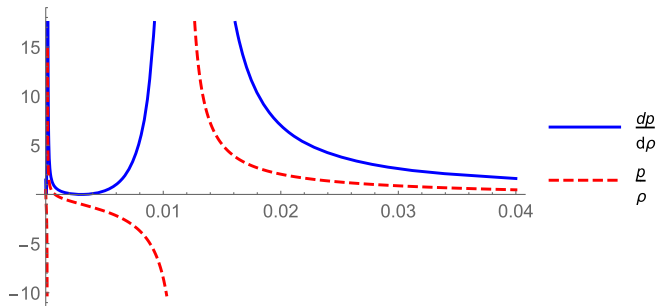


FIG. 13. Einstein: Sound speed squared $\frac{dp}{d\rho}$ and equation of state $\frac{p}{\rho}$ variation against radial value x .

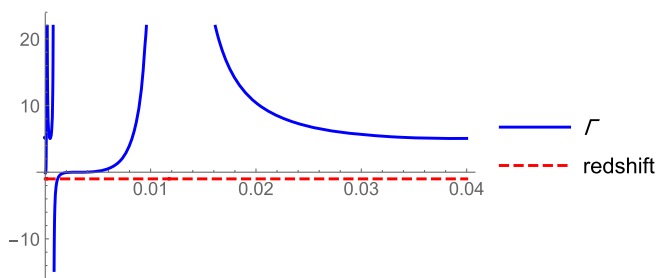


FIG. 14. Einstein: Adiabatic stability index Γ and redshift z variation against radial value x .

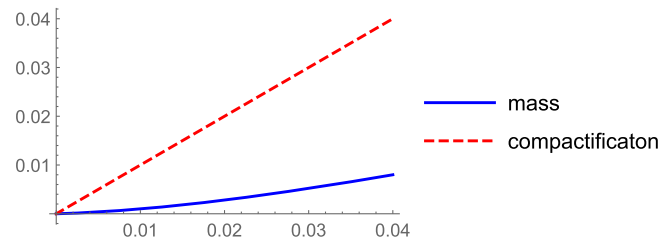


FIG. 15. Einstein: Mass and compactification index variation against radial value x .

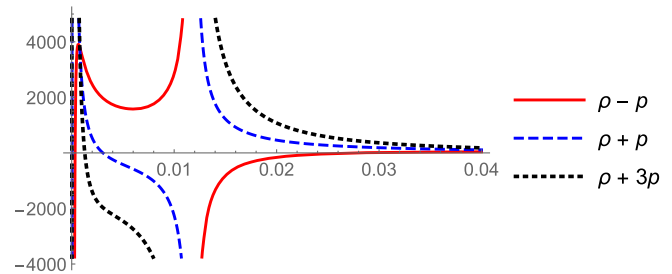


FIG. 16. Einstein: Energy conditions variation against radial value x .

however a central singularity appears. Figure 14 illustrates that the adiabatic stability index not in general satisfied and the surface gravitational redshift has the same value -1 as was the case for the EGB sphere. The mass profile and compactification index depicted in Fig. 15 are not remarkably different from the EGB case. According to Fig. 16 the energy conditions appear to hold outside of the center of the fluid distribution. In summary, the Einstein sphere is confined to a smaller radius than its EGB counterpart and suffers the critical defect of a central singularity. This suggests that the EGB model, with its higher curvature effects, has the potential to correct the physical behavior of static perfect fluid spheres in higher dimensions.

IX. CONCLUSION

We have investigated the consequences of a constant temporal potential in the case of the Einstein-Gauss-Bonnet fluid sphere. The linear spatial potential functions that emerged resulted in a constant density and constant pressure model that is deemed inconsistent with what is observed. The Einstein universe equation of state was generalized with the Gauss-Bonnet coupling playing a role. When the spatial gravitational potential was made constant an exact solution in terms of hypergeometric functions resulted. Since no exact solution in terms of elementary functions was realizable, a graphical qualitative analysis was undertaken and a comparison with the Einstein model was made when the higher curvature coupling was set to 0. In most respects it was found that the presence of higher curvature terms corrected certain defects in the Einstein ($\alpha = 0$) model. Specifically a persistent singularity in the Einstein model disappeared

when higher curvature terms were introduced. Additionally the EGB model permitted a 20-fold increase in the radial value. The investigation illustrates the severe consequences of the Gauss-Bonnet higher curvature effects in the construction of astrophysical objects. This strongly suggests that such effects should not be ruled out when attempting to extend Einstein's theory to accommodate observed phenomena that do not follow from the standard theory without the need to construe the existence of exotic matter fields.

ACKNOWLEDGMENTS

S. H. acknowledges the National Research Foundation of South Africa for financial support through Competitive Grant No. CSRP170419227721. S. D. M. acknowledges that this work is based upon research supported by the South African Research Chair Initiative of the Department of Science and Technology and the National Research Foundation.

-
- [1] B. P. Abbott *et al.*, *Phys. Rev. Lett.* **116**, 061102 (2016).
 - [2] D. N. Spergel, *Astrophys. J. Suppl. Ser.* **148**, 175 (2003).
 - [3] E. Komatsu, *Astrophys. J. Suppl. Ser.* **180**, 330 (2009).
 - [4] G. F. R. Ellis, H. van Elst, J. Murugan, and J.-P. Uzan, *Classical Quantum Gravity* **28**, 225007 (2011).
 - [5] G. F. R. Ellis, *Gen. Relativ. Gravit.* **46**, 1619 (2014).
 - [6] D. R. Finkelstein, A. A. Galiatdinov, and J. E. Baugh, *J. Math. Phys. (N.Y.)* **42**, 340 (2001).
 - [7] D. Lovelock, *J. Math. Phys. (N.Y.)* **12**, 498 (1971).
 - [8] D. Lovelock, *J. Math. Phys. (N.Y.)* **13**, 874 (1972).
 - [9] N. Dadhich, A. Molina, and A. Khugaev, *Phys. Rev. D* **81**, 104026 (2010).
 - [10] Z. Guo, N. Ohta, and T. Torii, *Prog. Theor. Phys. (Kyoto)*, **120**, 581 (2008).
 - [11] J. L. Blazquez-Salcedo, F. S. Khoo, and J. Kunz, *Phys. Rev. D* **96**, 064008 (2017).
 - [12] J. L. Ripley and F. Pretorius, *Classical Quantum Gravity* **36**, 134001 (2019).
 - [13] M. Iihoshi, *Gen. Relativ. Gravit.* **43**, 1571 (2011).
 - [14] D. D. K. Chow and Y. Pang, *Phys. Rev. D* **100**, 106004 (2019).
 - [15] N. Dadhich, K. Prabhu, and J. Pons, *Gen. Relativ. Gravit.* **45**, 1131 (2013).
 - [16] X. O. Camanho and N. Dadhich, *Eur. Phys. J. C* **76**, 149 (2016).
 - [17] N. Dadhich, S. Hansraj, and S. D. Maharaj, *Phys. Rev. D* **93**, 044072 (2016).
 - [18] N. K. Dadhich, S. Hansraj, and B. Chilambwe, *Int. J. Mod. Phys. D* **26**, 1750056 (2017).
 - [19] S. D. Maharaj, B. Chilambwe, and S. Hansraj, *Phys. Rev. D* **91**, 084049 (2015).
 - [20] S. Hansraj, B. Chilambwe, and S. D. Maharaj, *Eur. Phys. J. C* **75**, 277 (2015).
 - [21] B. Chilambwe, S. Hansraj, and S. D. Maharaj, *Int. J. Mod. Phys. D* **24**, 1550051 (2015).
 - [22] D. L. Wiltshire, *Phys. Rev. D* **38**, 2445 (1988).
 - [23] J. T. Wheeler, *Nucl. Phys.* **B268**, 737 (1986); **273**, 732 (1986).
 - [24] R. C. Myers and J. Simon, *Phys. Rev. D* **38**, 2434 (1988).
 - [25] Z. Kang, Y. Zhan-Ying, Z. De-Cheng, and Y. Rui-Hong, *Chin. Phys. B* **21**, 020401 (2012).
 - [26] J. Novak, M. Ozkan, Y. Pang, and G. Tartaglino-Mazzucchelli, *Phys. Rev. Lett* **119**, 111602 (2017).
 - [27] S. C. Davis, *Phys. Rev. D* **67**, 024030 (2003).
 - [28] M. Wright, *Gen. Relativ. Gravit.* **48**, 93 (2016).
 - [29] M. C. Durgapal and R. Bannerji, *Phys. Rev. D* **27**, 328 (1983).
 - [30] D. G. Boulware and S. Deser, *Phys. Rev. Lett.* **55**, 2656 (1985).
 - [31] L. K. Patel, N. P. Mehta, and S. D. Maharaj, *Nuovo Cimento* **112**, 1037 (1997).